EPR and ENDOR Characterization of Intermediates in the Cryoreduced Oxy-Nitric Oxide Synthase Heme Domain with Bound L-Arginine or N^G-Hydroxyarginine†

Roman Davydov,‡ Amy Ledbetter-Rogers,§ Pavel Martásek,||,⊥ Mikhail Larukhin,‡ Masanori Sono,# John H. Dawson,*,# Bettie Sue Siler Masters,*,|| and Brian M. Hoffman*,‡

Department of Chemistry, Northwestern University, Evanston, Illinois 60201, Department of Chemistry and Biochemistry, College of Charleston, Charleston, South Carolina 29424, Department of Chemistry and Biochemistry, University of South Carolina, Columbia, South Carolina 29208, Department of Biochemistry, The University of Texas Health Science Center at San Antonio, San Antonio, Texas 78229-3900, and Department of Pediatrics, Center of Integrative Genomics, 1st School of Medicine, Charles University, Prague, Czech Republic

Received May 2, 2002; Revised Manuscript Received June 25, 2002

ABSTRACT: Reconstitution of the endothelial nitric oxide synthase heme domain (NOS) with the catalytically noncompetent 4-aminotetrahydrobiopterin has allowed us to prepare at −40 °C the oxyferrous-NOS−substrate complexes of both L-arginine (Arg) and N^G-hydroxyarginine (NOHA). We have radiolytically cryoreduced these complexes at 77 K and used EPR and ENDOR spectroscopies to characterize the initial products of reduction, as well as intermediates that arise during stepwise annealing to higher temperatures. Peroxo-ferri-NOS is the primary product of 77 K cryoreduction when either Arg or NOHA is the substrate. Proton ENDOR spectra of this state suggest that the peroxo group is H-bonded to a [guanidinium−water] network that forms because the binding of O_2 to the ferroheme of NOS recruits H_2O. At no stage of reaction/annealing does one observe an EPR signal from a hydroperoxo-ferri state with either substrate. Instead, peroxo-ferri-NOS−substrate complexes convert to a product-state intermediate at the extremely low temperature of 165−170 K. EPR and proton ENDOR spectra of the intermediate formed with Arg as substrate support the suggestion that the reaction involves the formation and attack of Compound I. Within the time/temperature resolution of the present experiments, samples with Arg and NOHA as substrate behave the same in the initial steps of cryoreduction/annealing, despite the different acid/base characteristics of the two substrates. This leads us to discuss the possibility that ambient-temperature catalytic conversion of both substrates is initiated by reduction of the oxy-ferroheme to the hydroperoxo-ferriheme through a coupled proton−electron transfer from a heme-pocket reductant, and that Arg may provide the stoichiometrically second proton of catalysis.

Nitric oxide synthase (NOS)[1] catalyzes the formation of NO from L-arginine (Arg) in two dioxygen-activating stages, eq 1, the first of which produces N^G-hydroxyarginine (NOHA) and the second of which generates NO and citrulline (*1*−*6*).

$$\text{Arg} \xrightarrow[\text{NOS}]{O_2,\ 2e^-,\ 2H^+} \text{NOHA} \xrightarrow[\text{NOS}]{O_2,\ 1e^-,\ 1H^+} \text{citrulline} + NO^{\bullet} \quad (1)$$

Each stage begins with the reduction of ferri- to ferro-NOS, which binds dioxygen. The first stage has the stoichiometry of a 'classical' mixed-function hydroxylation, requiring a second electron and two protons to generate NOHA and water. The holoenzyme employs NADPH as the ultimate source of electrons, but dithionite also can act as an electron source to the NOS heme domain (*7*). Rapid-kinetic studies have provided evidence that tetrahydrobiopterin (H_4B), an essential cofactor bound in the heme pocket, then provides the 'second' electron, reducing the oxyferrous heme and generating a pterin radical (*8*−*10*), which must be rereduced prior to the next cycle. The reaction of NOHA to form NO and citrulline, the second stage of eq 1, does not stoichiometrically require a second electron, but nonetheless is thought to involve reduction of the oxyferrous heme, perhaps by the pterin as in step one, or else by NOHA itself (*7*, *11*).

It is widely thought that the reduction of the oxyferrous-NOS−Arg generates the peroxo-ferri-heme, which then proceeds through hydroperoxo-ferri-NOS to Compound I (Scheme 1), which is the actual hydroxylating intermediate. Precisely this scheme indeed applies to P450cam hydroxylations, for which it was first proposed (*12*−*15*), but it is not universal: the hydroxylating intermediate of heme oxygenase (HO) is the hydroperoxo-ferri form, not Compound I (*16*, *17*), and the peroxo-ferri form appears to be involved in a nitrile-to-amide conversion by P450 3A4 (*18*). In the

† We acknowledge grants from the National Institutes of Health [B.M.H. (HL13531), J.H.D. (GM26730), and B.S.S.M. (GM52419)], The Robert A. Welch Foundation [B.S.S.M. (AQ-1192)], and MSMT, Czech Republic [P.M. (LN 0VA079)].

‡ Northwestern University.
§ College of Charleston.
|| The University of Texas Health Science Center at San Antonio.
⊥ Charles University.
University of South Carolina.

[1] Abbreviations: NOS, endothelial nitric oxide synthase heme domain; Arg, L-arginine; NOHA, N^G-hydroxyarginine; H_4B, tetrahydrobiopterin; ENDOR, electron nuclear double resonance; EPR, electron paramagnetic resonance; HO, heme oxygenase; P450cam, cytochrome P450cam; NADPH, reduced nicotine adenine dinucleotide phosphate; EDTA, ethylenediaminetetraacetate.

10.1021/bi0260637 CCC: $22.00
Published on Web 07/25/2002

Scheme 1

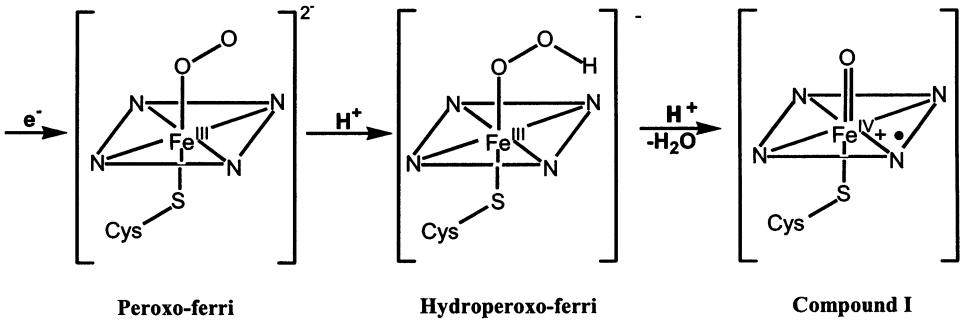

reactions of NOS, a pterin radical generated during the conversion of Arg has been detected by EPR (*8*, *19*), but until now no catalytically committed, activated-oxygen NOS heme intermediate has been detected or characterized for either stage.

In this report, we present EPR and ENDOR studies of activated-oxygen reaction intermediates formed in NOS. Reconstitution of the endothelial NOS heme domain with the catalytically noncompetent 4-amino-H_4B has allowed us to prepare relatively stable oxyferrous-NOS complexes of both the primary substrate, Arg, and NOHA, at −40 °C. We have radiolytically cryoreduced the oxy-heme of each complex at 77 K, and then characterized the initial product of reduction by EPR and ENDOR spectroscopies, as well as intermediates that arise during the relaxation that occurs during stepwise annealing to higher temperatures.

MATERIALS AND METHODS

The pterin-free endothelial NOS heme domain (denoted here simply as NOS) was prepared by trypsin cleavage of pterin-free full-length enzyme (*20*) in the presence of 0.5 mM Arg or NOHA. 4-Amino-H_4B and Arg or NOHA were added to concentrated heme domain samples (300−620 μM) to final concentrations of 0.5 mM (4-amino-H_4B) and 2 mM Arg or 1 mM NOHA. As monitored spectrophotometrically, oxy-NOS complexes were generated quantitatively in a spectrophotometric cell at −40 °C in buffer/ethylene glycol, 2:3 (v/v). The oxy complexes thus generated exhibited Soret absorption peaks at 429 and 427 nm in the presence of Arg and NOHA, respectively; detailed spectroscopic characterization of these oxy-NOS heme domain complexes will be published elsewhere.[2] Though the solutions were then rapidly transferred by microsyringe into narrow Q-band EPR tubes in a freezer box at −30 °C and rapidly frozen by immersion in liquid N_2, the samples prepared in this way nonetheless contained large amounts of the ferric form. The procedures for 77 K reduction of samples for EPR/ENDOR by γ-irradiation with a ^{60}Co source have been described, as have the procedures for subsequent annealing in 1 min steps, each at a specified temperature (*13*, *17*, *21*−*23*).

The 35 GHz EPR spectra are digital derivatives of rapid-passage dispersion-mode spectra, as described (*13*); ENDOR spectra were taken as described (*24*). Proton ENDOR spectra consist of two branches whose features are related by the formula: $\nu_\pm = \nu_H \pm A/2$, where ν_H is the proton Larmor frequency and A the magnitude of the hyperfine coupling parameter. As in our previous cryoreduction studies of oxy-ferrohemes (*13*, *17*), while the spectrum is comprised of ν_+ and ν_- branches symmetrically disposed about ν_H, the ν_+ branch is of lower intensity as a result of relaxation effects, and so we show only the ν_- region. Hyperfine tensors were determined from 2D sets of orientation-dependent ENDOR spectra, as described (*25*, *26*).

RESULTS

Oxy-NOS−*Arg*. Cryoreduction of oxy-NOS−Arg at 77 K produces a new rhombic, low-spin ferriheme EPR signal with $\mathbf{g} = [2.26, 2.16, \sim 1.95]$, which is seen in Figure 1 along with low-intensity features at $g = 2.44$ and 2.29 that belong to residual low-spin ferri-NOS, $\mathbf{g} = [2.44, 2.29, 1.89]$. This new signal, denoted as the $g_1 = 2.26$ species for its g_1 component, is essentially identical to those of the 'H-bonded peroxo-ferriheme' state created by cryoreduction of oxy-Hb/Mb (*23*, *27*−*30*) and oxy-P450(D251N) (*13*), and is assigned likewise.[3]

Figure 2 shows a 2D field/frequency set of ^{1}H ENDOR spectra of the cryoreduced oxy-NOS collected at numerous points across the EPR envelope of peroxo-ferri-NOS−Arg.[4] The spectrum taken at $g_1 = 2.26$ shows a signal from a strongly coupled proton [$A(g_1) \sim 11$ MHz] that is assigned to a proton hydrogen-bonded to the 'peroxo' moiety, as seen for the peroxo-ferri species of 77 K reduced oxy-Mb and oxy-Hb (*23*, *27*−*30*), and oxy-P450 D251N (*13*). The ν_- peak of the g_1 spectrum splits into two branches as the field is increased (g is decreased). The outer branch smoothly moves to a maximum offset from ν_H, corresponding to a maximum value of A, as the field is increased toward the vicinity of g_2; the offset of the inner branch decreases (decreasing A) until this branch merges with intense signals from other, mostly nonexchangeable protons. Spectra taken near g_3 again show a single ν_- peak.

Numerous simulations of the field-dependent pattern led to a best fit which employed a hyperfine tensor with components $\mathbf{A} = [\sim 4.5, \sim 5.3, 14.6(1)]$. The Euler angles

[2] A. Ledbetter-Rogers, P. Martásek, B. S. S. Masters, J. H. Dawson, and M. Sono, manuscript in preparation.

[3] The spectra obtained from 77 K reduced oxy-NOS-Arg/NOHA include superimposed signals from radicals produced in the matrix, but annealing to 155 K eliminates much of the radical signal without altering the NOS signals.

[4] As reflected in the figure, such experiments are constrained by an inability to collect spectra between roughly g_2 and g_3 because EPR signals from free radicals created by the irradiation overlap those of catalytic intermediates. Nonetheless, it is possible to trace enough of the field-dependent pattern for analysis.

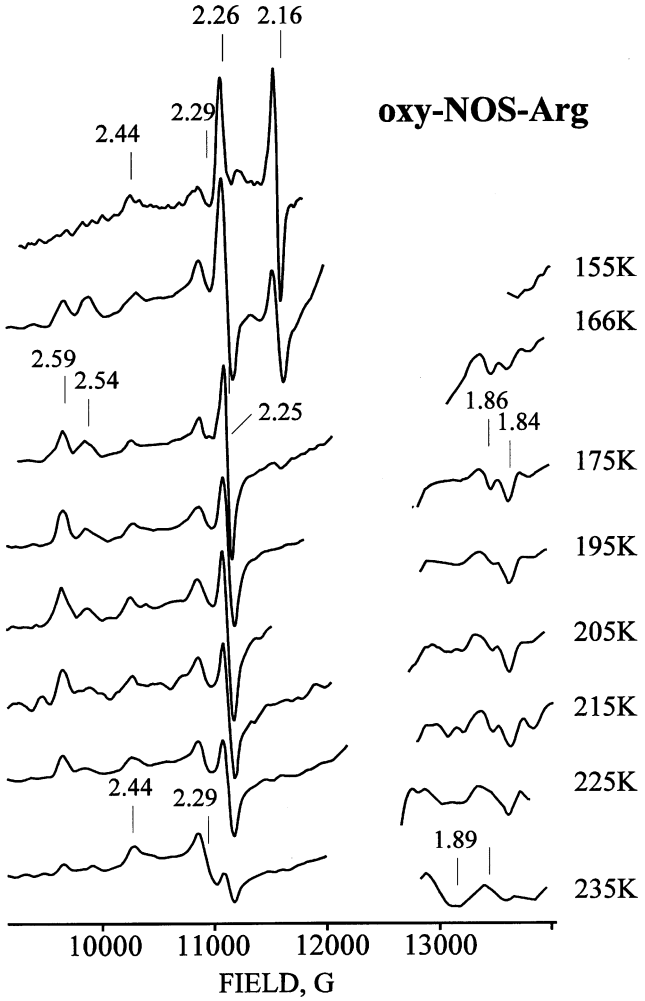

FIGURE 1: EPR spectra of the ternary complex of Arg, dioxygen, and ferro-NOS reduced radiolytically at 77 K. The dioxygen complex was prepared in the presence of 0.5 mM 4-amino-H_4B and 2.0 mM Arg in 60% ethylene glycol and 40% (v/v) 50 mM Tris buffer (pH 7.4) initially containing 0.1 mM EDTA and 10% (v/v) glycerol. Cryoreduction of these samples is estimated to create ca. 50 μM 'peroxoferri'-NOS. Spectra were taken after annealing at the indicated temperatures for 1 min. Conditions: 35.1 GHz; T = 2 K; spectra, collected with 100 kHz field modulation, are digital derivatives (see Materials and Methods); modulation amplitude 4 G.

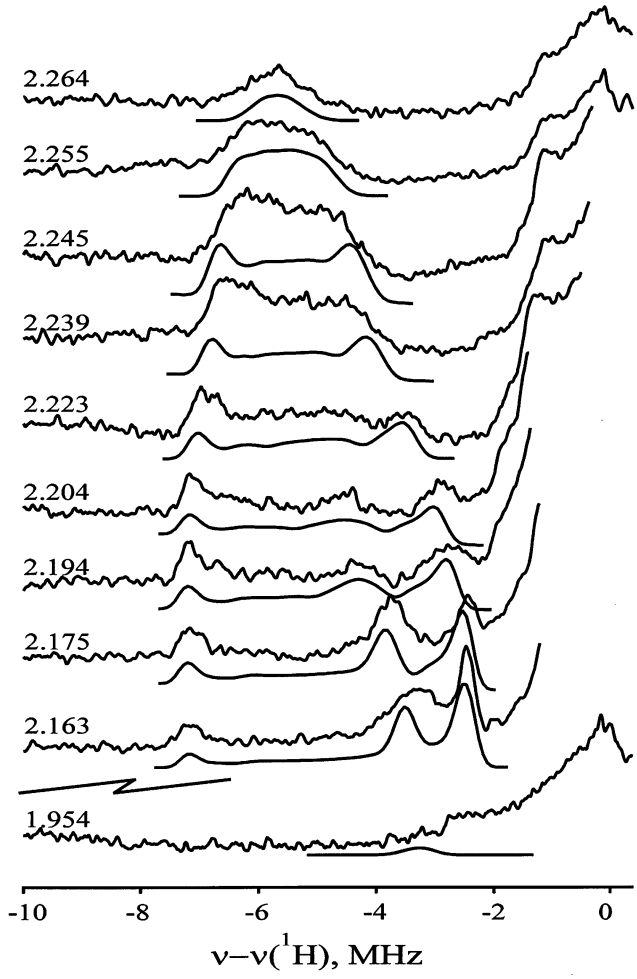

FIGURE 2: Orientation-selective, 2D field/frequency ^{1}H CW 35.2 GHz ENDOR patterns for 77 K peroxoferri-NOS−Arg prepared by 77 K cryoreduction. The spectra are comprised of doublets that are symmetric in frequency about ν_H according to eq 1; a commonly occurring asymmetry in *intensities* renders the ν_+ branch not only redundant according to the equation, but also less useful for measurements, and the figure presents only the ν_- branch of each spectrum. Dashed lines are simulations as described in the text. Conditions: 35.2 GHz; T = 2 K; field modulation 100 kHz; modulation amplitude 4 G; scan speed 1 MHz/s; 50 scans; 150 kHz broadening of RF excitation (*37*).

relating the **A**- and **g**-tensors are $\theta = 35(8)°$, $\phi = 34(4)°$; these are defined such that the polar angle, θ, is measured relative to the g_1 direction, which lies roughly along the heme normal, and the angle ϕ is defined as a rotation about g_1. As can be seen in Figure 2, this tensor gives a remarkably good representation of the experimental data. This tensor, with an isotropic contribution of $a = 8$ MHz and a dipolar term of $T = 3.3$ MHz, differs minimally from that we reported for peroxo-ferri-P450-D251N (*13*). However, in the earlier study, the signal from this exchangeable proton was more severely overlapped with other signals from other protons, and we declined to attempt to incorporate the azimuthal angle, ϕ, in those simulations. Encouraged by the present results, we have refit the older data and find that the 'H-bonded' proton of peroxo-ferri-P450-D251N has tensor components, **A** = [∼4, ∼5, 14.2(2)], and Euler angles relating the **A**- and **g**-tensors of $\theta = 38(4)°$, $\phi = 34(4)°$, values which are completely equivalent to those for NOS. Following the discussion given for the P450 system, it is likely that this ^{1}H signal of NOS comes from a proton that is H-bonded to the distal oxygen atom of the $Fe^{3+}-O_2^{2-}$ fragment.

Annealing. The appearance of the 'peroxo'-ferriheme signal upon 77 K reduction of oxy-NOS−Arg, rather than one from the hydroperoxo-ferric state, distinguishes NOS from the O_2-activating enzymes P450cam and HO. In those two cases, the peroxo form of the WT enzyme is not seen after 77 K reduction. Rather, the peroxo-ferriheme promptly accepts a proton from the distal-pocket H-bonding network at 77 K, and one detects only the signal of the hydroperoxo-ferri-enzyme, which has **g** ∼ [2.3, 2.17, 1.96] and is denoted the g_1-2.3 signal. Only when proton delivery in P450cam or HO is impeded by distal-pocket mutations (*13*, *17*) do these enzymes exhibit the $g_1 = 2.26$ peroxo-ferriheme signal following 77 K reduction. The peroxo-ferriheme states of the mutants of these two enzymes convert to the g_1-2.3 hydroperoxo-ferri-enzyme upon annealing to ∼180−200 K. Subsequent stepwise annealing of hydroperoxo-ferri-P450cam

(both WT and D251N mutants)(*13*) and of hydroperoxo-ferri-HO(WT)(*17*) to temperatures above ~200 K leads to formation of hydroxylated product.

Surprisingly, when peroxoferri-NOS−Arg is annealed from 77 K to the unusually low temperature of 165 K, its g_1-2.26 signal disappears *without* the observation of a g_1-2.3 signal from a hydroperoxo-ferriheme form. Instead, the annealing is accompanied by the appearance of two new EPR signals from low-spin ferriheme species with **g**-tensors, **g** = [2.59, 2.249, and 1.837] and [2.54, 2.249, and 1.858]; these are denoted as the g_1-2.59 and g_1-2.54 species, respectively (Figure 1).[5] The g_1-2.54 species appears to be the initial product, converting to the g_1-2.59 species upon annealing at 200 K; further stepwise annealing to 230 K causes the loss of the g_1-2.59 signal (Figure 1).

The *g*-2.59/2.54 signals resemble those of the primary P450cam−product complex, which has **g** = [2.62, 2.18, 1.865], and of partially relaxed forms of it which occur upon further annealing (*13*). In these species, the hydroxyl group of hydroxycamphor is coordinated to ferriheme in a non-equilibrium geometry. The similarity suggests that the NOS intermediates should likewise be assigned as containing a ferriheme to which the product of the reaction of the reactive NOS intermediate with the Arg substrate is bound in a nonequilibrium geometry. To test this possibility, ^{1}H ENDOR spectra were collected from the NOS g_1-2.54/2.59 intermediate (not shown). The spectra contain the signal of an exchangeable proton whose maximum splitting is no less than $A \sim 10-12$ MHz, compatible with the coupling seen for the hydroxyl proton of hydroxycamphor bound to ferri-P450 (*13*).

Oxy-NOS−NOHA. For comparison, analogous cryoreduction studies were performed with the oxy-NOS−NOHA complex. The 77 K reduction of oxy-NOS−NOHA also produces a peroxoferri species, and its **g**-tensor, **g** = [2.26, 2.152, ~1.95], is very similar to that of the peroxoferri-NOS formed with oxy-NOS−Arg as substrate (Figure 3). Annealing to ~165 K also causes peroxoferri-NOS−NOHA to disappear without the appearance of the g_1-2.3 signal from a hydroperoxoferri-NOS intermediate (Figure 3). Thus, *neither* oxy-NOS−Arg nor oxy-NOS−NOHA exhibits a signal from the hydroperoxo-ferriheme form during cryoreduction or subsequent annealing.

The reaction of bound NOHA according to eq 1 must produce a different product from that with Arg, and one would anticipate that annealing would generate a transient complex with distinct EPR properties. In fact, upon annealing to ~165 K, the g_1-2.26 signal generated from oxy-NOS−NOHA is replaced by a new intermediate whose **g**-tensor, **g** = [2.48, 2.23, 1.92], is similar to that of low-spin ferri-NOS (see above), to which it relaxes upon further annealing to ~190 K (Figure 3). The appearance of spectroscopically distinct transient intermediates when Arg or NOHA are present as substrates is consistent with the idea that these intermediates indeed represent nonequilibrium product complexes.

[5] We note that, as in the case of P450 and HO, spectra taken with the full field range of our magnet, ~1.6 T, showed no signal attributable to a high-valent NOS Compound I intermediate at any stage of the process.

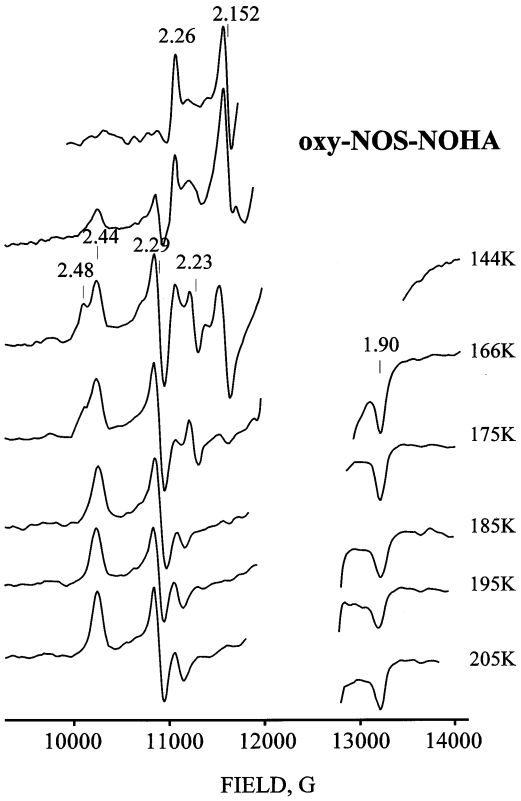

FIGURE 3: EPR spectra of the ternary complex of NOHA, dioxygen, and ferro-NOS (300 μM) reduced radiolytically at 77 K. Spectra were taken after annealing at the indicated temperatures for 1 min. The inset to the 144 K spectrum was prepared by subtracting the residual contribution from ferri-NOS−NOHA. Conditions: as in Figure 1, except that the sample contained 0.4 mM 4-amino-H_4B and 1 mM NOHA.

DISCUSSION

The present results show that 77 K reduction of the oxyferrous-NOS−substrate complexes with both Arg and NOHA leads to the formation of a g_1-2.26 'H-bonded-peroxo'-ferriheme species, such as have been characterized in studies of other cryoreduced oxy-hemoproteins. The EPR spectrum of this species depends slightly on the nature of the substrate bound, Arg or NOHA. A paramagnetic center produced by 77 K cryoreduction in general retains the structure of its diamagnetic precursor,[6] and thus these observations imply that the conformation of the heme−dioxygen moiety is modified by the bound substrate. This observation is consistent with the slight differences in Soret absorption maxima for the two substrate complexes [ref (*31*) and see above], and with the reported effect of these substrates on the EPR properties of the NO−ferrous-NOS complex (*32*).

Oxy-NOS is unique among the numerous oxy-hemoproteins studied by cryoreduction−EPR/ENDOR methods in not showing a signal from a hydroperoxoferri form. The peroxoferri form is the primary state observed upon 77 K cryoreduction of the oxy form of the O_2-*binding* proteins Mb/Hb, but subsequent annealing of these intermediates to temperatures of 180−190 K generates the hydroperoxoferri form by proton transfer, likely from the distal histidine (*27*).

[6] The exception to this rule is a low-temperature proton transfer, which does not occur here.

For the two O_2-*activating* enzymes we studied previously, P450cam (*13*) and HO (*17*), the initial species observed upon 77 K reduction of both their oxy complexes is the hydroperoxoferri form rather than the peroxoferri form, likely because there exists a distal-pocket H-bonding network containing a [−COOH···H_2O] motif that is prearranged to transfer a proton to the transiently formed peroxo moiety, and can do so even at 77 K [or below (*13*)]. In the P450cam (D251N) and HO (D141A, F) variants, the mutations disrupt the distal-pocket H-bond network. This prevents proton transfer at 77 K, and as a consequence, cryoreduction yields the peroxoferri form in both mutants. However, this form converts to the hydroperoxoferri-enzyme during annealing to 170−180 K. Both enzymes generate product upon further annealing to 210−220 K: for HO, the hydroperoxoferri state reacts directly to form product (*17*); for P450, this state produces a reactive Compound I intermediate which reacts rapidly, without accumulating, to form product (*13*). In contrast, peroxoferri-NOS is the primary product of 77 K cryoreduction when either Arg or NOHA is the substrate, and at no stage of reaction/annealing does one observe an EPR signal from a hydroperoxoferri state with either substrate.

Peroxoferri-NOS−Arg converts to the g_1-2.54 intermediate upon annealing to the extremely low temperature of 165−170 K. The characteristics of this intermediate support the assignment of it as a product complex, as follows. The EPR signal of the NOS g_1-2.54 intermediate is similar to that of the primary ferriheme product complex that appears upon hydroxylation of camphor by P450cam (*13*). In this complex, the hydroxyl group of the hydroxycamphor product is coordinated to iron in a nonequilibrium conformation, which relaxes in several stages to the equilibrium form upon further annealing. Moreover, the EPR spectrum of the NOS intermediate is essentially the same as those of complexes of *N*-hydroxyguanidines with 8-microperoxidase (**g** = [2.55, 2.26, 1.86] (*33*)).[7] Finally,[1]H ENDOR spectra of the NOS g = 2.54/2.59 intermediate show a proton signal whose maximum coupling, $A \sim 10-12$ MHz, is compatible with the coupling seen for the hydroxyl proton of hydroxycamphor bound to ferri-P450 (there is no nearby nonexchangeable proton on the guanidino group that could give such a large coupling). These comparisons suggest that the g_1-2.59/2.54 signals should be tentatively assigned to ferri-NOS complexes in which the NOHA product (eq 1) is bound in a nonequilibrium conformation with its hydroxyl group coordinated to the ferric ion. Further annealing to ∼230 K causes the disappearance of the g_1-2.59 signal, presumably because the coordinated hydroxyl of NOHA is released by the heme iron, as NOHA assumes its equilibrium conformation in which the hydroxyguanidino group of NOHA is not coordinated to the now pentacoordinate Fe(III).

The absence of a detectable signal from the hydroperoxoferri-NOS intermediate during cryoreduction/annealing of either oxy-NOS−substrate complex could, in principle, mean that it does not form, and that the peroxoferri-heme is the active species (*18*, *34*). However, if the g_1-2.54 signal indeed arises from a primary product state with the hydroxyl group of the NOHA product coordinated to the ferric ion,[6] then arguments first applied to P450cam (*13*) support the consensus conclusion (*1*−*6*) that the observed peroxoferri-NOS form proceeds to the hydroperoxoferri form and then to Compound I (Cpd I, Scheme 1), and that Cpd I is the hydroxylating species. Briefly, if Cpd I is the reactive species, the ferryl-oxygen becomes the hydroxyl-oxygen of NOHA, and an Fe−O−N linkage in the primary product state is a natural outcome. In contrast, if the reaction occurs by attack of a hydroperoxo moiety bound to the ferriheme, and the O−O bond does not break until after an N−O bond is formed to the remote O, then the bond breakage would generate NOHA and an aquo/hydroxo-ferriheme. Our data do not address the issue for the second stage of the reaction.

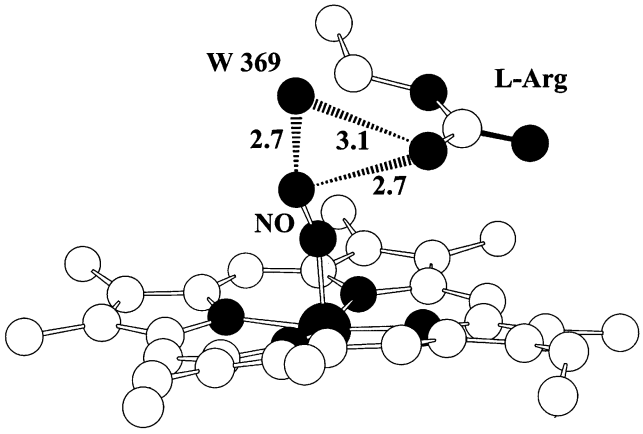

FIGURE 4: The NO−substrate ternary complex of the eNOS heme domain (pdb accession no. 1FOO)(*35*). The figure includes water 369; it deletes portions of the heme propionates, for clarity. Hatched lines indicate possible H-bonds; distances (Å).

Let us next consider possible sources of the two protons needed for monoxygenation, the first of which protonates the peroxo-ferriheme unit, the second of which activates the resulting hydroperoxo moiety for O−O bond cleavage. The crystal structure of the NO−NOS−Arg complex, which should be a reasonable structural surrogate for oxy-NOS, shows an H-bond from the terminal guanidinium moiety of Arg to the NO (*35*), and it has been suggested that the first proton of catalysis is supplied by the Arg (*36*). The first experimental evidence regarding this issue is provided by the ENDOR characterization of the proton that is H-bonded to the peroxo moiety of peroxoferri-NOS−Arg. This H-bond has essentially the same properties as those of the peroxoferri-P450cam(D251N), where the proton is associated with a water that is part of a H-bonding network (*14*). This suggests that the peroxo group in NOS is H-bonded to the water of a [guanidinium−water] 'network' that is present because the binding of O_2 to the ferroheme of NOS recruits H_2O. In fact, examination of the NO−NOS structure (pdb accession no. 1FOO)(*35*) shows the presence of a water (369) that is at H-bonding distance, about 2.7 Å, from the O atom of NO, and about 3.1 Å from NH1 of the substrate, while NH1 also is about 2.7 Å from the O of NO (Figure 4). This would further suggest that it is not Arg itself that provides a catalytic proton, but the [guanidinium−water] 'network'. The formation of product at ∼165−170 K, temperatures too low for major heme-pocket reorganization, further indicates that donors in the distal pocket can provide both protons of

[7] We recognize that this similarity is not conclusive, given that the proximal heme ligand is not the same in the two cases. The appropriate test of this assignment will be ENDOR studies with [^{15}N]arginine as substrate.

catalysis. An analogous scenario can be proposed to explain the cryoreduction/annealing results for the oxy-NOS−NOHA complex. For comparison, P450cam and HO also form product with protons donated from within the heme pocket, but only at temperatures above 210 K.

While it seems clear that Arg, or as we now suggest, a [guanidinium−H_2O] network, provides one of the two protons needed for dioxygen activation in the first stage of eq 1, our results can be viewed as opening to question whether this network provides the stoichiometrically first proton (*36*) or the second (*35*). If it were the first proton, then it must be viewed as surprising that the two oxy-NOS−substrate complexes behave equivalently during cryoreduction/annealing: NOHA is a potential proton donor whose pK_a is substantially lower than that of Arg (*33*). This and other considerations lead us to consider an alternate mechanism, where dioxygen activation involves a coupled electron/proton transfer in which a heme-pocket reductant transfers both the second electron and, ultimately, the 'first' proton of catalysis to the oxyferrous heme, perhaps by sequential transfer to the [guanidinium−H_2O]. This proposal might explain why the heme pocket of NOS is unable to protonate the peroxo-ferriheme formed by cryoreduction at 77 K: cryoreduction injects the second electron *without* an accompanying proton. With such a 'decoupling' of electron and proton delivery, the enzyme at 77 K is 'stuck' at the peroxo-ferriheme stage. Thermal activation to ∼165 K then permits the transfer of a proton from elsewhere in the pocket to generate the hydroperoxoferri-heme intermediate. This, in turn, apparently is sufficiently reactive at this temperature to accept a proton from the adjacent [guanidinium−H_2O] network, undergo O−O bond cleavage, and proceed along the catalytic cycle. It is now clear that the enzyme-bound tetrahydrobiopterin is the source of this electron during the chemical transformation of Arg (*8*, *19*), and this pterin is able to deliver *both* elements of an H atom. Moreover, this is true regardless of whether the resting-state, enzyme-bound pterin is in its neutral or cationic forms, H_4B or H_5B^+ (*6*)[8] (*8*, *19*, *20*).

A role for deprotonation of a heme-pocket moiety could explain the failure of H_2O_2 to support the first step of NOS catalysis. H_2O_2 *brings* both protons of catalysis, in addition to the two electrons and the 'O−O' moiety (eq 1).

Regarding the conversion of NOHA to L-citrulline and NO (Scheme 1), such a 'second' electron is not required stoichiometrically, but most proposed reaction mechanisms also incorporate an initiating reduction of the oxyferrous heme by a reductant within the heme pocket (*1*, *11*). Some schemes begin with reduction of the oxyferrous heme to form peroxoferri-NOS; others begin with delivery of the elements of 'H•', to generate the hydroperoxoferri-NOS intermediate (*11*). Regardless of whether the reductant is the pterin or NOHA itself, either can deliver the elements of H•.

Summary. Peroxoferri-NOS is the primary product of 77 K cryoreduction when either Arg or NOHA is the substrate. Proton ENDOR spectra of this state suggest that O_2 binding to the ferroheme of NOS recruits a H_2O, such that the peroxo group is H-bonded to a [guanidinium−water] network (see Figure 4). Among the cryoreduced oxyferrous-hemoproteins investigated to date, NOS is unique in that at no stage of reaction/annealing do we observe an EPR signal from a hydroperoxoferri state with either substrate. Instead, it appears that at ∼165 K the peroxoferri-heme is protonated, forming the hydroperoxoferri-NOS−substrate complex, but that this species does not accumulate and instead promptly converts to a product state at this extremely low temperature. EPR and proton ENDOR spectra of this state as formed with the Arg substrate support the consensus view that the reaction with Arg involves Compound I. Within the time/temperature resolution of the present experiments, samples with Arg and NOHA as substrates behave the same in the initial steps of cryoreduction/annealing, despite the different acid/base characteristics of the two substrates. This leads us to discuss the possibility that ambient-temperature catalytic conversion of both substrates is initiated by reduction of the oxy-ferroheme to the hydroperoxo-ferriheme through a coupled proton−electron transfer from a heme-pocket reductant, and that Arg may provide the stoichiometrically second proton of catalysis, not the first.

[8] The conclusion of Schmidt et al. (*19*) that the so-called 'H_4B radical' that builds up during room temperature mixing/rapid freeze−quench measurements of Arg hydroxylation (*8*) is in fact the $H_4B^{+\bullet}$ cation radical, would then imply that the resting-state enzyme binds H_5B^+, as suggested previously based on considerations of the NOS heme-pocket structure (*20*).

ACKNOWLEDGMENT

We thank Prof. T. L. Poulos for helpful discussions of NOS and its structure.

REFERENCES

1. Rosen, G. M., Tsai, P., and Pou, S. (2002) Mechanism of free-radical generation by nitric oxide synthase. *Chem. Rev. 102*, 1191−1199.
2. Roman, L. J., Martasek, P., and Masters, B. S. S. (2002) Intrinsic and extrinsic modulation of nitric oxide synthase activity. *Chem. Rev. 102*, 1179−1189.
3. Groves, J. T., and Wang, C. C. Y. (2000) Nitric oxide synthase: Models and mechanisms. *Curr. Opin. Chem. Biol. 4*, 687−695.
4. Poulos, T. L., Li, H., Raman, C. S., and Schuller, D. J. (2001) Structures of gas-generating heme enzymes: Nitric oxide synthase and heme oxygenase. *Adv. Inorg. Chem. 51*, 243−293.
5. Stuehr, D. J. (1999) Mammalian nitric oxide synthases. *Biochim. Biophys. Acta 1411*, 217−230.
6. Alderton, W. K., Cooper, C. E., and Knowles, R. G. (2001) Nitric oxide synthases: Structure, function and inhibition. *Biochem. J. 357*, 593−615.
7. Hurshman, A. R., and Marletta, M. A. (2002) Reactions catalyzed by the heme domain of inducible nitric oxide synthase: Evidence for the involvement of tetrahydrobiopterin in electron transfer. *Biochemistry 41*, 3439−3456.
8. Hurshman, A. R., Krebs, C., Edmondson, D. E., Huynh, B. H., and Marletta, M. A. (1999) Formation of a pterin radical in the reaction of the heme domain of inducible nitric oxide synthase with oxygen. *Biochemistry 38*, 15689−15696.
9. Bec, N., Gorren, A. F. C., Mayer, B., Schmidt, P. P., Andersson, K. K., and Lange, R. (2000) The role of tetrahydrobiopterin in the activation of oxygen by nitric-oxide synthase. *J. Inorg. Biochem. 81*, 207−211.
10. Wei, C.-C., Wang, Z.-Q., Wang, Q., Meade, A. L., Hemann, C., Hille, R., and Stuehr, D. J. (2001) Rapid kinetic studies link tetrahydrobiopterin radical formation to heme-dioxy reduction and arginine hydroxylation in inducible nitric-oxide synthase. *J. Biol. Chem. 276*, 315−319.
11. Huang, H., Hah, J.-M., and Silverman, R. B. (2001) Mechanism of nitric oxide synthase. Evidence that direct hydrogen atom abstraction from the O−H bond of N^G-hydroxyarginine is not relevant to the mechanism. *J. Am. Chem. Soc. 123*, 2674−2676.
12. Groves, J. T., and Han, Y. (1995) in *Cytochrome P450* (Ortiz de Montellano, P. R., Ed.) pp 3−48, Plenum Press, New York.
13. Davydov, R., Makris, T. M., Kofman, V., Werst, D. W., Sligar, S. G., and Hoffman, B. M. (2001) Hydroxylation of camphor by

reduced oxy-cytochrome P450cam: Mechanistic implications of EPR and ENDOR of catalytic intermediates in native and mutant enzymes. *J. Am. Chem. Soc. 123*, 1403−1415.
14. Schlichting, I., Berendzen, J., Chu, K., Stock, A. M., Maves, S. A., Benson, D. E., Sweet, B. M., Ringe, D., Petsko, G. A., and Sligar, S. G. (2000) The catalytic pathway of cytochrome P450cam at atomic resolution. *Science 287*, 1615−1622.
15. Sono, M., Roach, M. P., Coulter, E. D., and Dawson, J. H. (1996) Heme-containing oxygenases. *Chem. Rev. 96*, 2841−2887.
16. Ortiz de Montellano, P. R., and Wilks, A. (2001) Heme oxygenase structure and mechanism. *Adv. Inorg. Chem. 51*, 359−407.
17. Davydov, R., Kofman, V., Fujii, H., Yoshida, T., Ikeda-Saito, M., and Hoffman, B. (2002) Catalytic mechanism of heme oxygenase through EPR and ENDOR of cryoreduced oxy-heme oxygenase and its Asp140 mutants. *J. Am. Chem. Soc. 124*, 1798−1808.
18. Zhang, Z., Li, Y., Stearns, R. A., Ortiz de Montellano, P. R., Baillie, T. A., and Tang, W. (2002) Cytochrome P450 3A4-mediated oxidative conversion of a cyano to an amide group in the metabolism of pinacidil. *Biochemistry 41*, 2712−2718.
19. Schmidt, P. P., Lange, R., Gorren, A. C. F., Werner, E. R., Mayer, B., and Andersson, K. K. (2001) Formation of a protonated trihydrobiopterin radical cation in the first reaction cycle of neuronal and endothelial nitric oxide synthase detected by electron paramagnetic resonance spectroscopy. *JBIC, J. Biol. Inorg. Chem. 6*, 151−158.
20. Raman, C. S., Li, H., Martásek, P., Kral, V., Masters, B. S. S., and Poulos, T. L. (1998) Crystal structure of constitutive endothelial nitric oxide synthase: A paradigm for pterin function involving a novel metal center. *Cell 95*, 939−950.
21. Davydov, R., Valentine, A. M., Komar-Panicucci, S., Hoffman, B. M., and Lippard, S. J. (1999) An EPR study of the dinuclear iron site in the soluble methane monooxygenase from *Methylococcus capsulatus* (bath) reduced by one electron at 77 K: The effects of component interactions and the binding of small molecules to the diiron(III) center. *Biochemistry 38*, 4188−4197.
22. Davydov, R., Macdonald, I. D. G., Makris, T. M., Sligar, S. G., and Hoffman, B. M. (1999) EPR and ENDOR of catalytic intermediates in cryoreduced native and mutant oxy-cytochromes P450cam: Mutation-induced changes in the proton delivery system. *J. Am. Chem. Soc. 121*, 10654−10655.
23. Davydov, R. M., Yoshida, T., Ikeda-Saito, M., and Hoffman, B. M. (1999) Hydroperoxy-heme oxygenase generated by cryoreduction catalyzes the formation of α-meso-hydroxyheme as detected by EPR and ENDOR. *J. Am. Chem. Soc. 121*, 10656−10657.
24. Werst, M. M., Davoust, C. E., and Hoffman, B. M. (1991) Ligand spin densities in blue copper proteins by Q-band ^{1}H and ^{14}N ENDOR spectroscopy. *J. Am. Chem. Soc. 113*, 1533−1538.
25. Hoffman, B. M. (1991) Electron nuclear double resonance (ENDOR) of metalloenzymes. *Acc. Chem. Res. 24*, 164−170.
26. Hoffman, B. M., DeRose, V. J., Doan, P. E., Gurbiel, R. J., Houseman, A. L. P., and Telser, J. (1993) Metalloenzyme active-site structure and function through multifrequency cw and pulsed ENDOR. *Biol. Magn. Reson. 13*, 151−218.
27. Symons, M. C. R., and Petersen, R. L. (1978) Electron capture by oxyhaemoglobin: An ESR Study. *Proc. R. Soc. London, Ser. B B201*, 285−300.
28. Davydov, R. M. (1980) Optical and EPR spectroscopy of the electron adducts of oxymyoglobin and oxyhaemoglobin. *Biofizika 25*, 203−207.
29. Kappl, R., Höhn-Berlage, M., Hüttermann, J., Bartlett, N., and Symons, M. C. R. (1985) Electron spin and electron nuclear-double resonance of the $[FeO_2]^-$ centre from irradiated oxyhemo- and oxymyoglobin. *Biochim. Biophys. Acta 827*, 327−343.
30. Leibl, W., Nitschke, W., and Hüttermann, J. (1986) Spin-density distribution in the $[FeO_2]^-$ complex. Electron spin resonance of myoglobin single crystals. *Biochim. Biophys. Acta 870*, 20−30.
31. Gorren, A. C. F., Bec, N., Schrammel, A., Werner, E. R., Lange, R., and Mayer, B. (2000) Low-temperature optical absorption spectra suggest a redox role for tetrahydrobiopterin in both steps of nitric oxide synthase catalysis. *Biochemistry 39*, 11763−11770.
32. Migita, C. T., Salerno, J. C., Masters, B. S. S., Martásek, P., and Ikeda-Saito, M. (1997) Substrate binding-induced changes in the EPR spectra of the ferrous nitric oxide complexes of neuronal nitric oxide synthase. *Biochemistry 36*, 10987−10992.
33. Lefevre-Groboillot, D., Dijols, S., Boucher, J.-L., Mahy, J.-P., Ricoux, R., Desbois, A., Zimmermann, J.-L., and Mansuy, D. (2001) *N*-Hydroxyguanidines as new heme ligands: UV−visible, EPR, and resonance Raman studies of the interaction of various compounds bearing a C═NOH function with microperoxidase-8. *Biochemistry 40*, 9909−9917.
34. Newcomb, M., Shen, R., Choi, S.-Y., Toy, P. H., Hollenberg, P. F., Vaz, A. D. N., and Coon, M. J. (2000) Cytochrome P450-catalyzed hydroxylation of mechanistic probes that distinguish between radicals and cations. Evidence for cationic but not for radical intermediates. *J. Am. Chem. Soc. 122*, 2677−2686.
35. Li, H., Raman, C. S., Martásek, P., Masters, B. S. S., and Poulos, T. L. (2001) Crystallographic studies on endothelial nitric oxide synthase complexed with nitric oxide and mechanism-based inhibitors. *Biochemistry 40*, 5399−5406.
36. Crane, B. R., Arvai, A. S., Ghosh, D. K., Wu, C., Getzoff, E. D., Stuehr, D. J., and Tainer, J. A. (1998) Structure of nitric oxide synthase oxygenase dimer with pterin and substrate. *Science 279*, 2121−2126.
37. Hoffman, B. M., DeRose, V. J., Ong, J. L., and Davoust, C. E. (1994) Sensitivity enhancement in field-modulated cw ENDOR via RF bandwidth broadening. *J. Magn. Reson. 110*, 52−57.

BI0260637